Journal of Power Sources 417 (2019) 188–192

Contents lists available at ScienceDirect

Journal of Power Sources

journal homepage: www.elsevier.com/locate/jpowsour

Short communication

An easy-to-implement multi-point impedance technique for monitoring aging of lithium ion batteries

Xing Zhou[a,b], Zhengqiang Pan[a,*], Xuebing Han[b], Languang Lu[b], Minggao Ouyang[b,**]

[a] College of System Engineering, National University of Defense Technology, Changsha, 410072, China
[b] Department of Automotive Engineering, State Key Laboratory of Automotive Safety and Energy, Tsinghua University, Beijing, 100084, China

HIGHLIGHTS

- It requires impedance measurement at three frequency points only.
- The three frequency points are calibrated using DRT analysis.
- It can separate ohmic, contact and SEI resistances.
- Utility in monitoring battery aging is demonstrated.

GRAPHICAL ABSTRACT

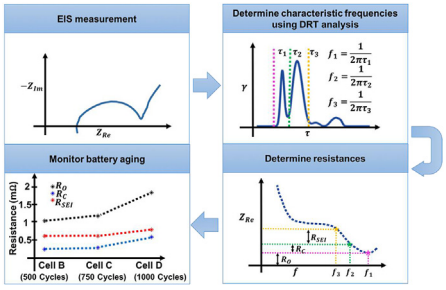

ARTICLE INFO

Keywords:
Lithium ion battery
Electrical vehicle
Electrochemical impedance
State of health
Battery monitoring and screening

ABSTRACT

The need for a quick yet informative technique for diagnosing the lithium-ion batteries is escalating. Conventional impedance-based diagnosis methods are usually time-demanding for a complete electrochemical impedance spectroscopy measurement and involve complicated calculations to extract battery information, which therefore have limited applications in battery monitoring. In this study, we propose a multi-point impedance technique, involving impedance measurement on three characteristic frequency points and being able to separate ohmic, contact and solid electrolyte interphase resistances. The characteristic frequency points are calibrated using distribution of relaxation time method. This multi-point impedance technique holds potential for large-scale high-throughput battery monitoring and screening.

1. Introduction

Electrochemical impedance spectroscopy (EIS) is a routine technique for characterization and diagnosis of lithium ion batteries. Through the interpretation of EIS data, physico-chemical processes exhibiting different time constants can be identified and physical parameters can be extracted for evaluating battery performance [1,2]. Equivalent circuit models (ECMs) are often used to analyze the EIS data by the complex nonlinear least square (CNLS) fitting method [3–12]. However, as put forward in Refs. [13,14], without a physically meaningful fitting model and good choice of initial parameters, the ECM approach cannot ensure reasonable identification of processes and estimation of parameters. To estimate the number of physical processes and generate good initial estimates of the ECM parameters, Huang et al. [14] proposed a graphical analysis of impedance data in Bode and Nyquist representations. An alternative, theoretically grounded approach is to adopt physics-based impedance models [15–21].

The distribution of relaxation time (DRT) method permits

* Corresponding author.
** Corresponding author.
E-mail addresses: panzhengqiang@nudt.edu.cn (Z. Pan), ouymg@tsinghua.edu.cn (M. Ouyang).

https://doi.org/10.1016/j.jpowsour.2018.11.087
Received 14 August 2018; Received in revised form 11 October 2018; Accepted 27 November 2018
Available online 04 December 2018
0378-7753/

deconvolution, with incomparable resolution, of the EIS data into multiple relevant polarization processes in a wide frequency range [22,23]. Illig et al. [14] employed the DRT method to separate polarizations related with the solid-state diffusion, the charge transfer reaction and the contact resistance between active materials and current collectors of a $LiFePO_4$ cathode. A follow-up work from the same group further determined the specific time constants and polarization resistances of these processes [25]. Moreover, using a reference electrode, Illig et al. [26] is able to separate polarization losses associated with cathode and anode, respectively. Recently, the DRT method was applied to compare different cathodes in 18650 cells [27].

Usually, the DRT method requires EIS measurement over a wide frequency range which is often conducted by using a commercial electrochemical workstation, and involves complicated calculation which is often conducted off-line. These two limitations restrict the application of the DRT method in large-scale high-throughput battery monitoring and screening. As one of initial attempts to amend this issue, Love et al. [28,29] proposed a single-point impedance diagnosis for monitoring the overcharge abuse and state of health (SOH) of $LiCoO_2$ cells. The impedance response at a single designated frequency, nearly invariant within the whole state of charge (SOC) range, was presumed to be associated with the solid electrolyte interphase (SEI) film. Albeit being simple, this single-point impedance method hinges on an overall impedance quantity with individual contributions smeared out altogether.

In this work, a multi-point impedance technique that is easy to complement, simple to calculate, and capable of distinguishing the ohmic resistance, the contact resistance and the SEI resistance, is proposed for monitoring and screening of lithium ion batteries. The remaining part of this paper is organized as follows. Section two presents breakdown of polarization losses into ohmic, electric contact, SEI and charge transfer parts using the DRT method. Informed from above detailed polarization breakdown, in section three, three characteristic frequency points are chosen and the utility of the multi-point impedance technique is demonstrated. Section four concludes major findings.

2. Separation of polarization losses

Based on previous studies [23,30], the polarization losses in lithium ion cells are divided into five parts: (1) the ohmic resistance R_O, (2) the contact resistance R_C, (3) the SEI resistance R_{SEI}, (4) the charge transfer resistance R_{CT}, and (5) the diffusion resistance R_D. R_O is associated with ionic conduction in the electrolyte and electronic conduction in the electrode. R_C results from the electric contact between active materials and the current collector. R_{SEI} is related with the transport of lithium ions through the SEI film. R_{CT} is connected with the activation of the electrochemical reactions at the electrode/electrolyte interface. R_D arises from the diffusion of lithium ions in the electrolyte and solid active particles (see Refs. [19,20] for detailed discussion on their differences). These polarization resistances are of different dependence on the state of charge (SOC[1]) and temperature. R_O, R_C and R_{SEI} are nearly unrelated with the SOC, because the corresponding polarization losses are independent on the concentration of lithium ions in the solid active particles. On the contrary, R_{CT} and R_D are of highly SOC-dependent due to the dependence of the charge transfer and diffusion processes on the concentration in the solid active particles. On the other hand, the activation energies of the polarization resistances are also related with the corresponding physical mechanisms. Jamnik et al. [31] proposed that the contact impedance is not a pure resistance but a parallel connection of a resistance and a capacitor, embodied as a high-frequency semicircle in the Nyquist plot. Furthermore, the contact impedance may manifest a time constant distribution, as there is a distribution in the separation distance in between, as shown in Fig. 1. By virtue of this, the contact resistance can be distinguished from the ohmic resistance which has a single extremely small time constant and can be safely regarded as a pure resistance. The DRT method is employed to distinguish these resistances.

Four commercial large-format $LiNi_{1/3}Mn_{1/3}Co_{1/3}O_2$/graphite pouch cells (denoted as cell A-D) were employed in the experiment. The experimental procedures and original EIS data are presented in the supporting materials. For meaningful DRT analysis, the diffusion impedance in the low frequency range is eliminated, as proposed by Illig [24,25]. Afterwards, the remaining impedance spectra are deconvolved by virtue of the DRT method, see details in the supporting materials.

The DRT results of cell A for a wide SOC range between 100% and 0% at 25 °C are shown in Fig. 2(a). Four individual peaks can be clearly identified, which are denoted as P1-4. Each peak corresponds to an individual process. For an individual process with the time constant ranging from τ_L to τ_U, the polarization resistance R_p can be calculated by Eq. (1), as derived in the supporting materials,

$$R_p = \int_{\tau_L}^{\tau_U} \gamma(\tau) d\tau \tag{1}$$

where γ represents the distribution of the polarization losses, and $\gamma(\tau)d\tau$ is therefore the resistance contributed by the polarization losses having a time constant between τ and $\tau + d\tau$. Regarding the ohmic resistance, it corresponds to an extremely small time constant, thus, cannot be directly read from Fig. 2. Instead, we can determine the ohmic resistance as a model parameter by fitting Eq. (B.1) in the supporting materials to the impedance data.

As shown in Fig. 2(a), the SOC dependence of P1 and P2 is weak. On the contrary, P3 and P4 are highly dependent on the SOC. Especially when the SOC is lower than 20%, P3 and P4 increase rapidly with decreasing of the SOC. Therefore, P3 and P4 are related with the charge transfer resistance. However, further distinction between the anode and cathode is not attempted in this study.

Fig. 2(b) shows the DRT results of cell A at four temperatures from 15 °C to 45 °C at 50% SOC. The four peaks are temperature dependent. In a decreasing order of temperature, the time constants of P2-4 move to the right, and the polarization resistances of P1-4 increase significantly. Furthermore, P2 is much more sensitive to the temperature compared with P1. It is reported that the SEI resistance is highly dependent on the temperature [32], while the contact resistance is believed to be weakly temperature-dependent. Therefore, we attribute P1 and P2 to the contact and SEI impedance, respectively.

Fig. S4 exhibits the relations between the four resistances and temperature. Linear relationships are observed between the logarithm of the resistances and the inverse of absolute temperature. From the linear relationships using the Arrhenius law, activation energies of the four resistances are 0.09 eV for R_O, 0.16 eV for R_C, 0.79 eV for R_{SEI} and 0.67 eV for R_{CT} respectively. Ref. [24] reported 0.14 eV for R_O, 0.06 eV for R_C, 0.72 eV for R_{SEI} and 0.45 eV for R_{CT} for a $LiFePO_4$ cathode. Information obtained from polarization breakdown is summarized in Fig. 3.

3. Multi-point impedance technique

The polarization resistances exhibit different dependence on the SOC. Specifically, the charge transfer and diffusion resistances are highly SOC-dependent. Development of an impedance-based monitoring and screening technique, which is the objective of this study, shall employ a resistance that is largely SOC-independent, otherwise we need to adjust the battery SOC which is time and cost consuming. Therefore, this work utilizes the former three resistances for monitoring battery aging. For instance, increase in R_O often mirrors electrolyte decomposition, and increase in R_C reflects contact loss from current

[1] In this work, SOC is defined by $\frac{C_N - Q_D}{C_N}$, where C_N is the nominal capacity, and Q_D is the capacity discharged from a fully charged battery cell.

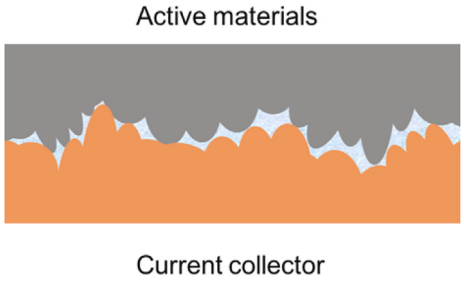

Fig. 1. Schematic illustration of the contact between active materials and the current collector.

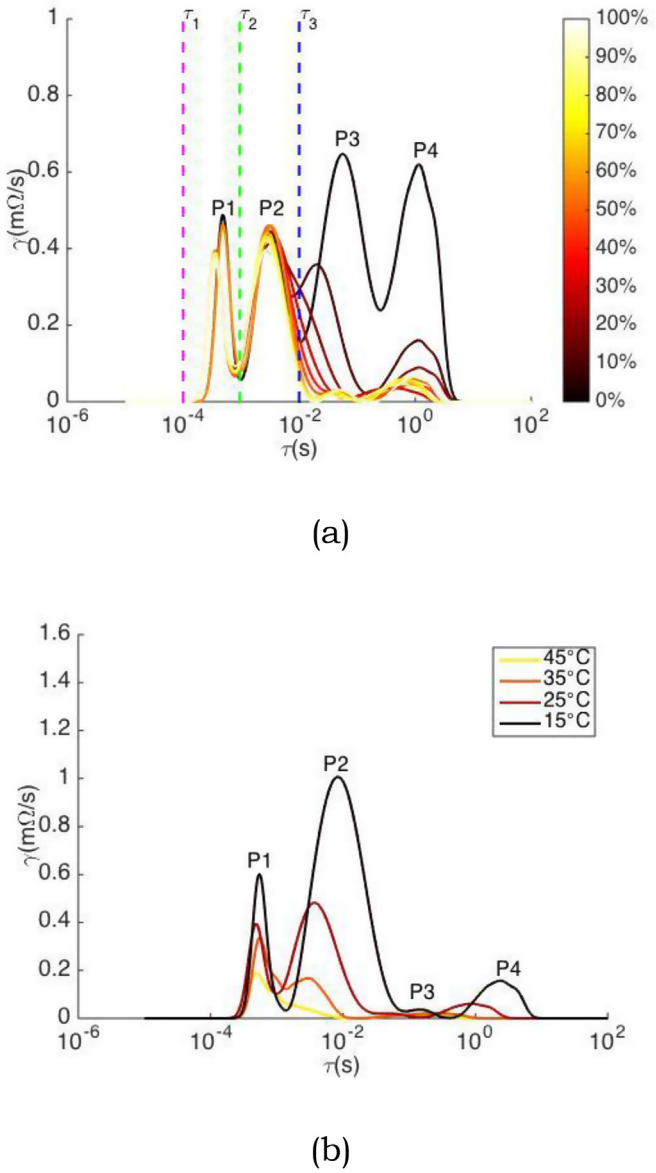

Fig. 2. DRT results of a cell (a) at different SOCs at 25 °C; (b) at different temperatures at 50% SOC.

collector corrosion, and increase in R_{SEI} presents SEI growth, which is believed to be the major cause of battery degradation, respectively [33].

The key issue then becomes how to determine these three resistances quickly at a minimal cost. Though the polarization resistances can be obtained by the DRT method, EIS measurement over a wide frequency range and complicated calculation restrict its application in large-scale battery monitoring. For quick battery monitoring, an alternative approach is proposed to approximate the polarization resistances obtained by the DRT method.

The overall impedance at a certain frequency is contributed, to different degrees, by all polarization losses. There are characteristic frequencies at which one or several of the processes are fully developed. We choose three such characteristic frequency points f_1, f_2 and f_3, that the impedance $Z(f_1)$ is almost exclusively contributed by the ohmic loss, $Z(f_2)$ by the sum of the ohmic and contact loss, and $Z(f_3)$ by the sum of the ohmic, contact and SEI loss. Then, it is straightforward to calculate the ohmic, contact and SEI resistance below,

$$R_O \approx Real(Z(f_1)) \tag{2}$$

$$R_C \approx Real(Z(f_2)) - Real(Z(f_1)) \tag{3}$$

$$R_{SEI} \approx Real(Z(f_3)) - Real(Z(f_2)) \tag{4}$$

Characteristic frequency points f_i are calculated from characteristic time constants τ_i obtained from the DRT analysis in section 2, via $f_i = 1/2\pi\tau_i$. As shown in Fig. 2(a) at 25 °C, we have $\tau_1 = 10^{-4}$s, $\tau_2 = 9.5 \times 10^{-4}$s and $\tau_3 = 10^{-2}$s. The polarization loss with a time constant smaller than τ_1 corresponds to the ohmic resistance, while the contact and SEI resistance dominates within the range from τ_1 to τ_2 and τ_2 to τ_3, respectively.

We further find that the same set of τ_i applies for different cells of the same kind at different aging levels, making it possible for this technique to diagnose battery aging. The DRT results of cell B (500 cycles), cell C (750 cycles) and cell D (1000 cycles) are presented in Fig. S3, where τ_1, τ_2 and τ_3 obtained from cell A are marked out. It is concluded that the characteristic time constants for the three cells with different aging levels are quite close to that of cell A. (From the DRT results, the explicit characteristic time constants are 10^{-4}s, 10^{-3}s and 10^{-2}s for cell B, 10^{-4}s, 10^{-3}s and 10^{-2}s for cell C, and 10^{-4}s, 9×10^{-4}s and 9×10^{-3}s for cell D.)

After determining f_i, the question at the present is how well the resistances calculated from Eqs. (2)–(4) at three characteristic frequencies represent the 'true' values extracted from the DRT analysis over a full frequency range. As shown in Fig. 4(a), the resistances calculated from the three-point impedance technique agree with their 'true' values in the whole SOC range, with an error less than 10% shown in Fig. 4(b). In addition, Fig. 4(c) verifies that this technique is also applicable to accurately (with an error less than 10% shown in Fig. 4(d)) predict the resistances for cells at different aging levels.

4. Conclusion

This work is contributed to propose a multi-point impedance technique for monitoring aging of lithium ion batteries at a significantly reduced cost. After initial calibration of the characteristic frequencies using the DRT method, the technique is able to estimate the ohmic, contact and SEI resistance at different aging levels, requiring impedance measurement at several impedance points only. Another merits of this technique is that it is insensitive to the cell SOC, as a result, unaffordable costs in adjusting the SOC in conventional methods are exempted. In the future work, we are to develop a low-cost device based on this technique, and implement it for large-scale high-throughput battery monitoring and screening.

Acknowledgement

This work is supported by the National Natural Science Foundation of China under the Grant No. U1564205, International Science & Technology Cooperation Program of China under contract No. 2016YFE0102200 and Beijing Natural Science Foundation under the Grant No.3184052. The authors are indebted to Dr. Jun Huang at

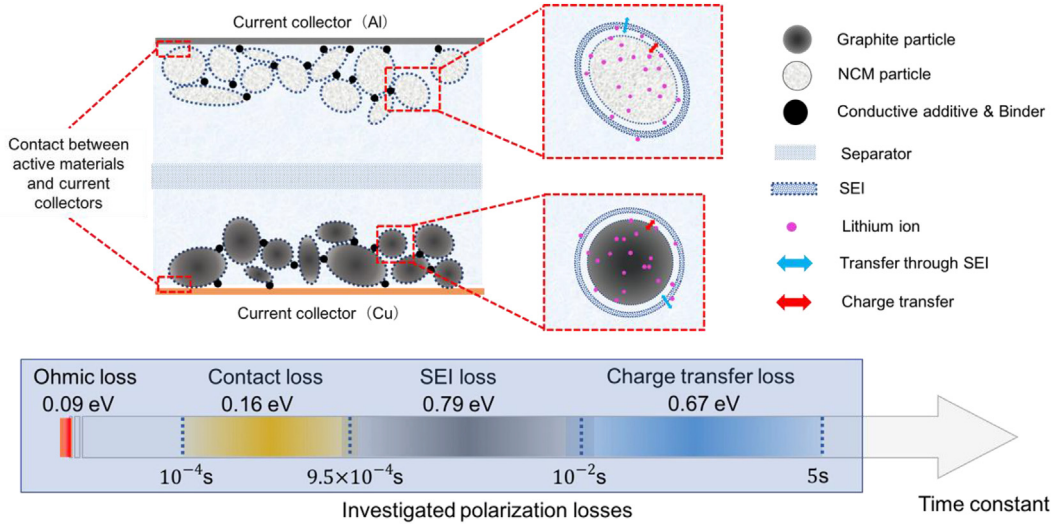

Fig. 3. Schematic illustration and breakdown of polarization in a NCM lithium ion cell at 25 °C.

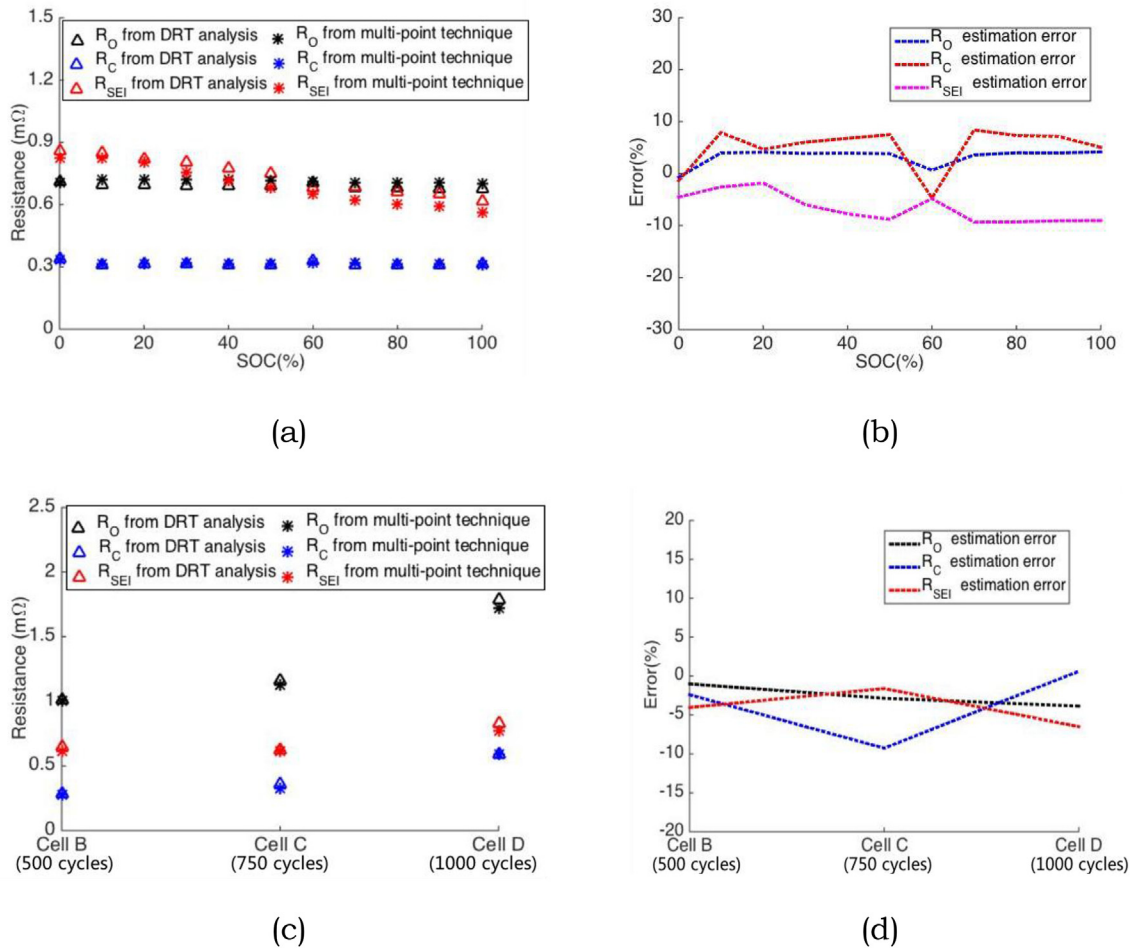

Fig. 4. Comparison between the polarization resistances calculated from the DRT method and that from the multi-point impedance technique. (a) Cell A with SOC variation at 25 °C; (b) estimation errors for cell A; (c) cell B, cell C and cell D at 50%SOC and 25 °C; (d) estimation errors for cell B, cell C and cell D.

Central South University for helpful discussion and language editing.

Appendix A. Supplementary data

Supplementary data to this article can be found online at https://doi.org/10.1016/j.jpowsour.2018.11.087.

References

[1] E. Barsoukov, J.R. Macdonald (Eds.), Impedance Spectroscopy: Theory, Experiment, and Applications, Wiley-Interscience, New York, 2005.
[2] M.E. Orazem, B. Tribollet, Electrochemical Impedance Spectroscopy, John Wiley & Sons, 2011.
[3] J.E.B. Randles, Kinetics of rapid electrode reactions, Discuss. Faraday Soc. 1 (1971)

11–19, https://doi.org/10.1039/DF9470100011.
[4] M.D. Levi, D. Aurbach, Impedance of a single intercalation particle and of non-homogeneous, multilayered porous composite electrodes for Li-ion batteries, J. Phys. Chem. B 108 (2004) 11693–11703, https://doi.org/10.1021/jp0486402.
[5] U. Tröltzsch, O. Kanoun, H.R. Tränkler, Characterizing aging effects of lithium ion batteries by impedance spectroscopy, Electrochim. Acta 51 (2006) 1664–1672, https://doi.org/10.1016/j.electacta.2005.02.148.
[6] C. Huang, K. Huang, S. Liu, Y. Zeng, L. Chen, Storage behavior of LiNi1/3Co1/3Mn1/3O2/artificial graphite Li-ion cells, Electrochim. Acta 54 (2009) 4783–4788, https://doi.org/10.1016/j.electacta.2009.02.018.
[7] Y. Zhang, C. Wang, Cycle-life characterization of automotive lithium-ion batteries with LiNiO 2 cathode, J. Electrochem. Soc. 156 (7) (2009) A527–A535, https://doi.org/10.1149/1.3126385.
[8] D. Andre, M. Meiler, K. Steiner, H. Walz, T. Soczka-Guth, D.U. Sauer, Characterization of high-power lithium-ion batteries by electrochemical impedance spectroscopy. II: Modelling, J. Power Sources 196 (2011) 5349–5356, https://doi.org/10.1016/j.jpowsour.2010.07.071.
[9] K. Jalkanen, J. Karppinen, L. Skogström, T. Laurila, M. Nisula, K. Vuorilehto, Cycle aging of commercial NMC/graphite pouch cells at different temperatures, Appl. Energy 154 (2015) 160–172, https://doi.org/10.1016/j.apenergy.2015.04.110.
[10] Q.A. Huang, Y. Shen, Y. Huang, L. Zhang, J. Zhang, Impedance characteristics and diagnoses of automotive lithium-ion batteries at 7.5% to 93.0% state of charge, Electrochim. Acta 219 (2016) 751–765, https://doi.org/10.1016/j.electacta. 2016.09.154.
[11] Y. Leng, S. Ge, D. Marple, X.-G. Yang, C. Bauer, P. Lamp, C.-Y. Wang, Electrochemical cycle-life characterization of high energy lithium-ion cells with thick Li(Ni 0.6 Mn 0.2 Co 0.2)O 2 and graphite electrodes, J. Electrochem. Soc. 164 (2017) A1037–A1049, https://doi.org/10.1149/2.0451706jes.
[12] C. Pastor-Fernández, K. Uddin, G.H. Chouchelamane, W.D. Widanage, J. Marco, A comparison between electrochemical impedance spectroscopy and incremental capacity-differential voltage as Li-ion diagnostic techniques to identify and quantify the effects of degradation modes within battery management systems, J. Power Sources 360 (2017) 301–318, https://doi.org/10.1016/j.jpowsour.2017.03.042.
[13] J. Ross MacDonald, Three to six ambiguities in immittance spectroscopy data fitting, J. Phys. Condens. Matter 24 (2012), https://doi.org/10.1088/0953-8984/24/17/175004.
[14] J. Huang, Z. Li, B.Y. Liaw, J. Zhang, Graphical analysis of electrochemical impedance spectroscopy data in Bode and Nyquist representations, J. Power Sources 309 (2016) 82–98, https://doi.org/10.1016/j.jpowsour.2016.01.073.
[15] M. Doyle, J.P. Meyers, J. Newman, Computer simulations of the impedance response of lithium rechargeable batteries, J. Electrochem. Soc. 147 (2000) 99, https://doi.org/10.1149/1.1393162.
[16] J.P. Meyers, M. Doyle, R.M. Darling, J. Newman, The impedance response of a porous electrode composed of intercalation particles, J. Electrochem. Soc. 147 (2000) 2930, https://doi.org/10.1149/1.1393627.
[17] G. Sikha, R.E. White, Analytical expression for the impedance response for a lithium-ion cell, J. Electrochem. Soc. 155 (2008) A893, https://doi.org/10.1149/1.2976359.
[18] T.G. Zavalis, M. Klett, M.H. Kjell, M. Behm, R.W. Lindström, G. Lindbergh, Aging in lithium-ion batteries: model and experimental investigation of harvested LiFePO4 and mesocarbon microbead graphite electrodes, Electrochim. Acta 110 (2013) 335–348, https://doi.org/10.1016/j.electacta.2013.05.081.
[19] J. Huang, J. Zhang, Theory of impedance response of porous electrodes: simplifications, inhomogeneities, non-stationarities and applications, J. Electrochem. Soc. 163 (2016) A1983–A2000, https://doi.org/10.1149/2.0901609jes.
[20] J. Huang, Z. Li, J. Zhang, S. Song, Z. Lou, N. Wu, An analytical three-scale impedance model for porous electrode with agglomerates in lithium-ion batteries, J. Electrochem. Soc. 162 (2015) A585–A595, https://doi.org/10.1149/2.0241504jes.
[21] J. Huang, H. Ge, Z. Li, J. Zhang, An agglomerate model for the impedance of secondary particle in lithium-ion battery electrode, J. Electrochem. Soc. 161 (2014) E3202–E3215, https://doi.org/10.1149/2.027408jes.
[22] H. Schichlein, H. Schichlein, E. Ivers-tiffe, E. Ivers-tiffe, M. Voigts, A. Kru, H. Schichlein, A.C. Mu, A. Müller, M. Voigts, Deconvolution of electrochemical impedance spectra for the identification of electrode reaction mechanisms in solid oxide fuel cells, J. Appl. Electrochem. 32 (2002) 875–882, https://doi.org/10.1023/A:1020599525160.
[23] M. Ender, J. Illig, J.P. Schmidt, D. Klotz, E. Ivers-tiffée, Identification of reaction mechanisms in lithium-ion batteries by deconvolution of electrochemical impedance spectra, The 15th International Meeting on Lithium Batteries - IMLB 2010, The Electrochemical Society, 2010Abstract #784.
[24] J. Illig, M. Ender, T. Chrobak, J.P. Schmidt, D. Klotz, E. Ivers-Tiffee, Separation of charge transfer and contact resistance in LiFePO4-cathodes by impedance modeling, J. Electrochem. Soc. 159 (2012) A952–A960, https://doi.org/10.1149/2.030207jes.
[25] J.P. Schmidt, T. Chrobak, M. Ender, J. Illig, D. Klotz, E. Ivers-tiffée, Studies on LiFePO4 as cathode material using impedance spectroscopy, J. Power Sources 196 (2011) 5342–5348, https://doi.org/10.1016/j.jpowsour.2010.09.121.
[26] J. Illig, J.P. Schmidt, M. Weiss, A. Weber, E. Ivers-tiffée, Understanding the impedance spectrum of 18650 LiFePO4-cells, J. Power Sources 239 (2013) 670–679, https://doi.org/10.1016/j.jpowsour.2012.12.020.
[27] B. Manikandan, V. Ramar, C. Yap, P. Balaya, Investigation of physico-chemical processes in lithium-ion batteries by deconvolution of electrochemical impedance spectra, J. Power Sources 361 (2017) 300–309, https://doi.org/10.1016/j.jpowsour.2017.07.006.
[28] C.T. Love, K. Swider-lyons, Impedance diagnostic for overcharged lithium-ion batteries, Electrochem. Solid State. 15 (2012) 53–56, https://doi.org/10.1149/2.014204esl.
[29] C.T. Love, M.B.V. Virji, R.E. Rocheleau, K.E. Swider-lyons, State-of-health monitoring of 18650 4S packs with a single-point impedance diagnostic, J. Power Sources 266 (2014) 512–519, https://doi.org/10.1016/j.jpowsour.2014.05.033.
[30] A. Nyman, T.G. Zavalis, R. Elger, M. Behm, G. Lindbergh, Analysis of the polarization in a Li-ion battery cell by numerical simulations, J. Electrochem. Soc. 157 (2010) A1236, https://doi.org/10.1149/1.3486161.
[31] M. Gaberscek, J. Moskon, B. Erjavec, R. Dominko, J. Jamnik, The importance of interphase contacts in Li ion electrodes: the meaning of the high-frequency impedance arc, Electrochem. Solid State Lett. 11 (2008) A170, https://doi.org/10.1149/1.2964220.
[32] N.S. Spinner, C.T. Love, S.L. Rose-pehrsson, S.G. Tuttle, Electrochimica acta expanding the operational limits of the single-point impedance diagnostic for internal temperature monitoring of lithium-ion batteries, Electrochim. Acta 174 (2015) 488–493, https://doi.org/10.1016/j.electacta.2015.06.003.
[33] J. Vetter, P. Novák, M.R. Wagner, C. Veit, K.C. Möller, J.O. Besenhard, M. Winter, M. Wohlfahrt-Mehrens, C. Vogler, A. Hammouche, Ageing mechanisms in lithium-ion batteries, J. Power Sources 147 (2005) 269–281, https://doi.org/10.1016/j.jpowsour.2005.01.006.